PHYSICAL REVIEW B VOLUME 56, NUMBER 18 1 NOVEMBER 1997-II

Inverse melting in a system with positive heats of formation

Hai Yang Bai, C. Michaelsen, and R. Bormann
Institute for Materials Research, GKSS-Research Center, Max-Planck-Strasse, D-21502 Geesthacht, Germany
(Received 7 July 1997)

Supersaturated body-centered-cubic Fe-W solid solutions with positive heats of formation were prepared by cosputtering and mechanical alloying over a wide concentration range. Upon annealing, these solid solutions were observed to undergo amorphization in the range of 20–37 at. % W. For $Fe_{70}W_{30}$ and $Fe_{67}W_{33}$ the transformation was polymorphous, indicating an inverse melting behavior. A thermodynamic analysis of the Fe-W system, which was carried out using the calculation-of-phase-diagrams method, supported that inverse melting is energetically possible in the Fe-W system. The results demonstrate that inverse melting can also occur in systems with positive heats of amorphous phase formation. [S0163-1829(97)51042-3]

In the Ti-Cr alloy system,[1] it has been demonstrated that at low temperature undercooled liquid or amorphous phases can become thermodynamically more stable than a (metastable) crystalline state. Such a behavior indicates that a second melting point can occur at low temperature, and that a metastable crystal can melt polymorphously upon cooling if the formation of equilibrium phases is avoided.[2] Accordingly, this phenomenon has been termed inverse melting, and the temperature below which the undercooled liquid or amorphous phase is thermodynamically more stable than the crystalline state has been termed inverse melting temperature.[3] In contrast to normal melting, which is an endothermic transformation, inverse melting is exothermic.

Subsequent investigations have revealed that inverse melting occurs in several transition-metal alloy systems, all of which exhibit negative heats of mixing in the liquid state and therefore can develop chemical and topological ordering upon undercooling.[4] Examples of systems where inverse melting could be experimentally confirmed include Ti-Cr,[1,5,6] Nb-Cr,[7,8] Ta-Cr,[9] and Mo-Zr.[10] In addition to these systems, our recent investigations have indicated that the Fe-W system may be a further candidate for inverse melting,[11,12] although Fe and W exhibit a positive heat of mixing in the liquid state at high temperature and in the body-centered-cubic (bcc) solid solution.

In this paper, we demonstrate that a polymorphous transformation from a crystalline phase to an amorphous phase can be obtained in supersaturated bcc Fe-W solid solutions prepared by codeposition. This provides experimental evidence that the inverse melting phenomenon is not restricted to alloys with negative heats of amorphous phase formation but can also be found in a system with positive heats of amorphous phase formation. The experimental results are interpreted in terms of a thermodynamic analysis of the Fe-W system which was performed using the calculation-of-phase diagrams (CALPHAD) method.

Fe-W alloy films with compositions ranging from 13–67 at. % W were deposited by cosputtering from elemental targets onto Si single-crystal substrates kept at room temperature by water cooling. The deposition was carried out using argon (7N) at a pressure of 0.37 Pa. The base vacuum was typically 1.2×10^{-7} Pa before deposition. The Fe-W alloy films were about 4 μm in total thickness, allowing the preparation of freestanding samples for the differential scanning calorimetry (DSC) experiments by peeling the films from the substrates. Mechanical alloying of Fe and W powder blends were performed with a planetary mill (for experimental details, see Refs. 11 and 12). Different compositions ranging from 20–30 at. % W were milled up to 1400 h. O and N levels remained unchanged after milling and stayed typically below 0.2 wt. %. No Fe contamination was detected. The DSC measurements were performed under argon atmosphere, either in a Perkin Elmer DSC 7 or in a high-temperature calorimeter of type Netzsch DSC 404. X-ray diffraction (XRD) measurements were performed using a Siemens D5000 powder diffractometer with Cu-K_α radiation.

The XRD measurements of the Fe-W alloy films showed the formation of bcc solid solution phases in the entire composition range investigated, except for compositions around 45 at. % where an amorphous phase was observed. DSC traces of the bcc phase with compositions <41 at. % W showed a broad exothermal peak from 500–750 °C and a sharp exothermal peak at about 900 °C. As an example, a DSC trace of a $Fe_{73}W_{27}$ film sample is shown in Fig. 1(a), taken at a heating rate of 40 K/min. XRD investigations performed after the DSC measurements indicated that the low-temperature DSC peak is associated with the amorphization of the bcc solid solutions, whereas the high-temperature peak is due to crystallization of the amorphous phases. XRD patterns of a $Fe_{70}W_{30}$ film sample before and after different heat treatments are shown in Fig. 2. Figure 2(a) shows an as-sputtered $Fe_{70}W_{30}$ solid solution. The lattice parameter of the bcc phase was determined to be 0.2979 nm. This value is slightly higher than the linear interpolation between pure Fe and W, in agreement with the positive heat of mixing of Fe and W in the bcc phase. Figure 2(b) shows the XRD pattern of the $Fe_{70}W_{30}$ sample after heating at a rate of 40 K/min to 720 °C. It can be seen that a diffuse halo typical of an amorphous phase developed upon heating, indicating a polymorphous transformation from the bcc solid solution to the amorphous phase. Figure 2(c) shows the XRD pattern of the $Fe_{70}W_{30}$ sample after heating to 1200 °C. It shows that the amorphous phase has crystallized into Fe and the intermetallic compound Fe_7W_6 which are the equilibrium phases at 1200 °C. Figure 3 shows that amorphization occurred in the

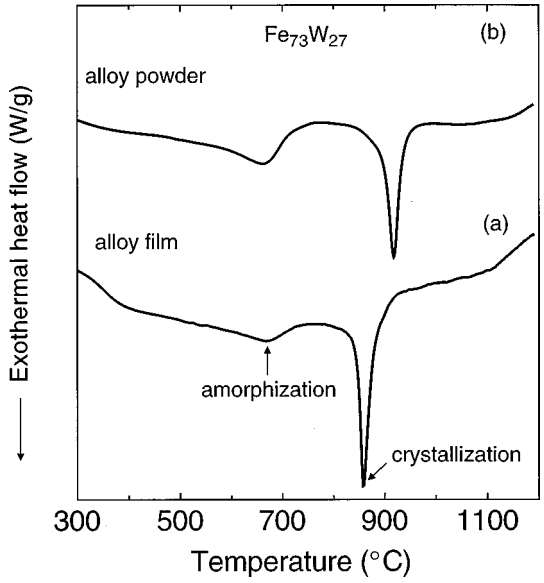

FIG. 1. DSC traces of $Fe_{73}W_{27}$ samples, taken at a heating rate of 40 K/min to 1200 °C. (a) Alloy film sample; (b) alloy powder sample.

Fe-W solid solutions with different compositions upon heating to 720 °C with heating rates of 50, 40, 10, and 4 K/min, respectively. The different heating rates were used because the transformation temperatures increased with W content. (The application of a higher annealing temperature is unreasonable, as the inverse melting temperatures of these alloys decrease with W content from 820 to about 600 °C, see below.) The Fe-rich sample ($Fe_{74}W_{26}$) showed decomposition of the bcc solid solution into an amorphous phase, bcc Fe and a small amount of the Fe_7W_6 compound upon heating. The samples with 30 and 33 at. % W showed a polymorphous transformation from the bcc solid solution to the amorphous phase, with a slight shift of the amorphous halo to lower angles upon increasing W concentration. The W-rich sample ($Fe_{63}W_{37}$) showed an almost complete amorphization and a small amount of bcc solid solution. The residual solid solution has a slightly higher W content than the initial bcc solid solution.

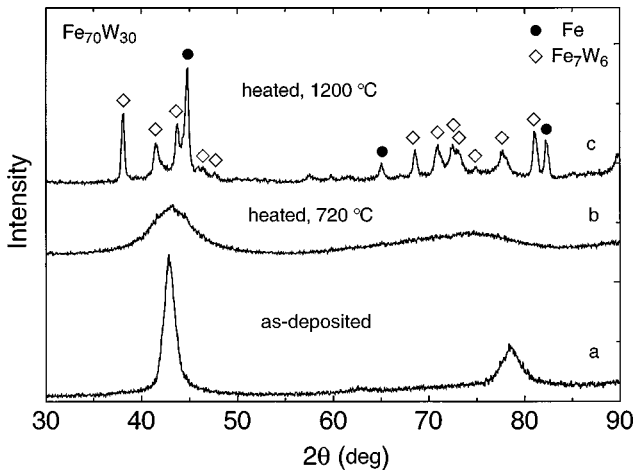

FIG. 2. XRD patterns of the $Fe_{70}W_{30}$ film sample before and after heat treatments, performed at a heating rate of 40 K/min.

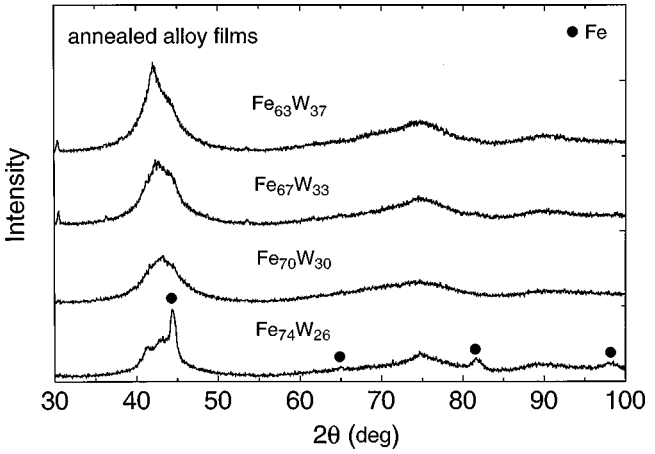

FIG. 3. XRD patterns of the $Fe_{74}W_{26}$, $Fe_{70}W_{30}$, $Fe_{67}W_{33}$, and $Fe_{63}W_{37}$ film samples after heating to 720 °C.

Bcc solid solutions with concentrations of 20, 25, and 27 at. % W were also obtained by mechanical alloying, whereas for 30 at. % W the formation of an amorphous phase was observed. Upon heating, the bcc alloy transformed into an amorphous phase. A DSC trace of a $Fe_{73}W_{27}$ alloy powder sample is shown in Fig. 1(b), taken at a heating rate of 40 K/min. Compared to the results obtained from alloy films with similar compositions a reasonable similarity is observed. Figure 4 shows XRD patterns of the Fe-W powders with different compositions after heating to 800 °C. Only a small portion of Fe precipitated in the $Fe_{73}W_{27}$ powder upon heating as the transformation from the bcc to the amorphous phases is almost polymorphous. These results are consistent with those obtained from the cosputtered films and demonstrate that the transformation into the amorphous phase is not determined by processing or by a specific microstructure.

The thermodynamic functions of the Fe-W system were determined by the CALPHAD method, as described in Ref. 12. The calculations were based on data of the equilibrium phase diagram, available thermodynamic data from literature, and enthalpy data from our earlier investigation of the Fe-W system.[11,12] The amorphous phase is treated as an extension of the undercooled liquid at low temperatures. The

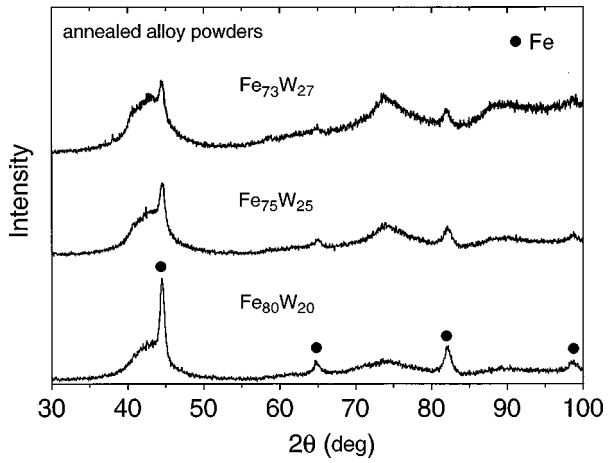

FIG. 4. XRD patterns of the bcc $Fe_{80}W_{20}$, $Fe_{75}W_{25}$, and $Fe_{73}W_{27}$ powder samples after heating to 800 °C, taken at a heating rate of 20 K/min.

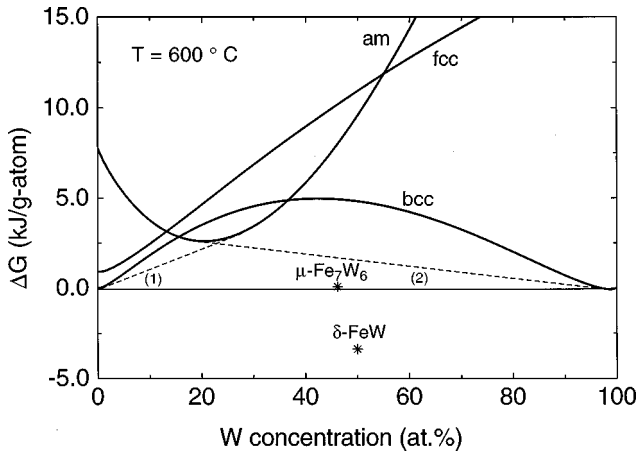

FIG. 5. Gibbs energy curves of the bcc and fcc solid solutions, the amorphous phase, and the μ-Fe_7W_6 and δ-FeW compounds at 600 °C. Dashed lines (1) and (2) are common tangents between the amorphous phase and Fe-rich or W-rich bcc solid solution, respectively. Reference states are bcc Fe and bcc W.

calculation considers the temperature dependence of the excess specific heat for the undercooled liquid and its change at the glass transition temperature. Consequently, the thermodynamic functions of the liquid and the amorphous phase are mainly determined by the phase equilibria of the liquid phase at high temperatures and by crystallization enthalpies of the amorphous phase at different compositions.[13] In addition, magnetic contributions on the Fe-rich side were also considered in the present evaluation. Figure 5 shows the Gibbs energy curves of the bcc and fcc solid solutions, the amorphous phase, and the μ-Fe_7W_6 and δ-FeW compounds at 600 °C. It is worth noting that all phases except the δ phase exhibit positive heats of formation. It can be seen that the amorphous phase has a lower Gibbs energy than the bcc solid solution in the composition range 16–37 at. % W, i.e., the amorphous phase is energetically preferred over the bcc phase in this concentration range. This is in agreement with our experimental results which showed amorphization in this concentration range.

Figure 6 displays Gibbs energy curves of the bcc phase and the liquid/amorphous phase as a function of temperature at a composition of $Fe_{70}W_{30}$. It can be seen that two points of intersection between the Gibbs energies of these two

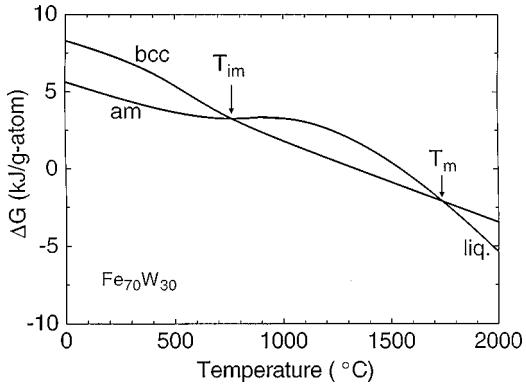

FIG. 6. Gibbs energy curves of the bcc phase and the liquid/amorphous phase as a function of temperature at a composition of $Fe_{70}W_{30}$. Reference states are bcc Fe and bcc W.

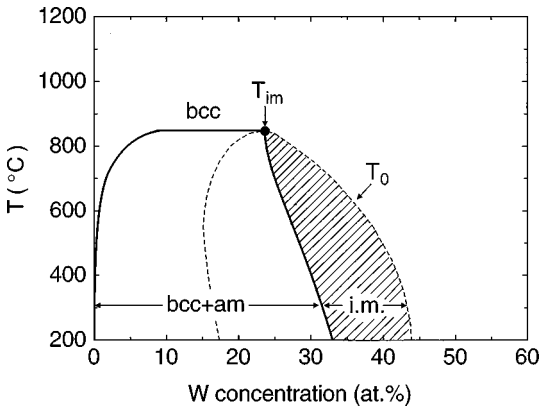

FIG. 7. T_0 curves (dashed lines) and metastable equilibria (solid lines) of the amorphous phase and the bcc phase.

phases exist, the first being the usual polymorphous melting point at high temperature, and the second being the inverse melting point at 760 °C. Below 760 °C a driving force exists for a polymorphous transformation from the bcc to the amorphous phase.

Figure 7 shows T_0 curves derived from equal energy points confining the region in which the amorphous phase has a lower Gibbs energy than the bcc phase. In addition, Fig. 7 shows metastable equilibria between the amorphous phase and the Fe-rich bcc phase obtained from the common tangents applied to the Gibbs energy curves of these two phases. Usually, there are two common tangents possible between the Gibbs energy curves of the amorphous phase and that of the bcc solid solution. One is between the amorphous phase and the Fe-rich bcc phase and the other is between the amorphous phase and W-rich bcc phase, as denoted for $T = 600$ °C by dashed lines (1) and (2) in Fig. 5. However, it is obvious from Fig. 5 that the amorphous phase, as a result of its positive Gibbs energy of formation, would not form if precipitation of both the Fe-rich and the W-rich could occur simultaneously. Since this is in disagreement with our experimental observation of amorphous phase formation, we can conclude that the formation of one of these two bcc phases is kinetically suppressed. In fact, our experimental results indicate such a kinetic suppression: for example, during heating of the Fe-rich solid solution, Fe precipitated from the bcc phase while precipitation of W did not occur. With this constraint, a metastable equilibrium diagram between the amorphous phase and the Fe-rich bcc phase was constructed in Fig. 7. The two-phase field so obtained ends at approximately 850 °C in a horizontal line. This feature is the result of the fact that the Gibbs energies of the bcc and amorphous phases become almost identical at this temperature in a concentration range of 8–24 at. % W.

Our experimental results are in good agreement with the calculated T_0 and the metastable equilibrium lines: for W concentrations equal or lower than 27 at. % we observed precipitation of Fe parallel to amorphization. This indicates that metastable equilibria between these phases may develop in Fe-rich samples. For higher W concentrations, Fe precipitation is energetically not favorable during amorphization and precipitation of W is not observed. This allows a polymorphous transformation of the bcc solid solution into an amorphous phase for temperatures below 850 °C to occur.

However, such a transformation is only energetically possible within a concentration-temperature region limited by the T_0 line. As a result, polymorphous amorphization is expected to occur only in the shaded region denoted ''i.m.'' (inverse melting), for instance, from 27–37 at. % W at $T = 600\ ^\circ$C and from 25–33 at. % W at $T = 700\ ^\circ$C. This is in perfect agreement with our experiments. For higher W content above 33 at. %, driving force for a polymorphous transformation exists only at lower temperatures, where transformation kinetics are too slow for these compositions. Therefore only partial amorphization is observed.

In conclusion, by preparing homogeneous bcc solid solutions by cosputtering and mechanical alloying of Fe and W, we have demonstrated that a polymorphous transformation from a crystalline to an amorphous phase occurred by annealing of supersaturated bcc Fe-W solid solutions in the concentration range of 30–33 at. % W. For lower W contents, two-phase mixtures consisting of the amorphous and Fe-rich bcc phases were observed. The inverse melting phenomenon agrees well with the thermodynamics of the Fe-W system. These results demonstrate that inverse melting can occur also in systems with positive heats of amorphous phase formation.

One of the authors (Hai Yang Bai) is grateful for the financial support of the Alexander von Humboldt Foundation in Germany. Thanks also go to T. Klassen and C. Gente for valuable discussions. The financial support of the Deutsche Forschungsgemeinschaft DFG-SP Unterkühlte Metallschmelzen, Az: Bo 691/5 is gratefully acknowledged.

[1] Z. H. Yan, T. Klassen, C. Michaelsen, M. Oehring, and R. Bormann, Phys. Rev. B **37**, 8520 (1993).
[2] R. Bormann, Mater. Sci. Eng. A **179/180**, 31 (1994).
[3] A. L. Greer, J. Less-Common Met. **140**, 327 (1988).
[4] R. Bormann, C. Michaelsen, W. Sinkler, and Th. Pfullmann, Mater. Sci. Forum **225-227**, 5 (1996).
[5] C. Michaelsen, Z. H. Yan, and R. Bormann, J. Appl. Phys. **73**, 2249 (1993).
[6] W. Sinkler, C. Michaelsen, and R. Bormann, Phys. Rev. B **55**, 2874 (1997).
[7] C. Michaelsen, M. Oehring, and R. Bormann, Appl. Phys. Lett. **65**, 318 (1994).
[8] C. Michaelsen, W. Sinkler, Th. Pfullmann, and R. Bormann, J. Appl. Phys. **80**, 2156 (1996).
[9] C. Michaelsen (unpublished).
[10] W. Sinkler and R. Bormann (unpublished).
[11] Hai Yang Bai, C. Michaelsen, W. Sinkler, and R. Bormann, Mater. Sci. Forum **235-238**, 361 (1997).
[12] Hai Yang Bai, C. Michaelsen, and R. Bormann (unpublished).
[13] R. Bormann and K. Zöltzer, Phys. Status Solidi A **131**, 69 (1992).